Three thymine/adenine binding modes of the ruthenium complex Λ-[Ru (TAP)2(dppz)]2+ to the G-quadruplex forming sequence d(TAGGGTT) shown by X-ray crystallography

Article

Accepted Version

McQuaid, K. ORCID: https://orcid.org/0000-0002-3222-5584, Hall, J. P. ORCID: https://orcid.org/0000-0003-3716-4378, Baumgaertner, L., Cardin, D. J. and Cardin, C. J. ORCID: https://orcid.org/0000-0002-2556-9995 (2019) Three thymine/adenine binding modes of the ruthenium complex Λ-[Ru (TAP)2(dppz)]2+ to the G-quadruplex forming sequence d(TAGGGTT) shown by X-ray crystallography. Chemical Communications, 55. pp. 9116-9119. ISSN 1359-7345 doi: 10.1039/C9CC04316K Available at https://centaur.reading.ac.uk/84918/

Three thymine-adenine binding modes of the ruthenium complex Λ-[Ru (TAP)2(dppz)]2+ to the G-quadruplex forming sequence d(TAGGGTT) shown by X-ray crystallography

Article

Accepted Version

COMMUNICATION

Three thymine/adenine binding modes of the ruthenium complex Λ-[Ru(TAP)$_2$(dppz)]$^{2+}$ to the G-quadruplex forming sequence d(TAGGGTT) shown by X-ray crystallography

Received 00th January 20xx,
Accepted 00th January 20xx

DOI: 10.1039/x0xx00000x

Kane T. McQuaid,[a,c] James P. Hall [b,c] John A Brazier[b], Lena Baumgartner[a], David J. Cardin[a] and Christine J. Cardin*[a]

Λ-[Ru(TAP)$_2$(dppz))$^{2+}$ was crystallised with the G-quadruplex-forming heptamer d(TAGGGTT). Surprisingly, the complex is not in contact with any G-quartet surface, even though there are four unique binding sites. Two complexes stabilise cavities formed from terminal TA and TT mismatched pairs. A third shows kinking by a TAP ligand between TT linkages, while the fourth shows sandwiching of a dppz ligand between a TA/TA quadruplex and a TT mismatch, stabilised by an additional TA basepair stacking interaction on a TAP surface. Overall, the structure shows an unexpected affinity for thymine, and suggests models for G-quadruplex loop binding.

Currently there are no structural models for the interactions of monomeric ruthenium polypyridyl complexes with the loop regions of nucleic acid assemblies such as the G-quadruplex and the i-motif. The biological importance of the G-quadruplex has become clear in the last few years,[1] and it has become an important drug target.[2] These single stranded assemblies are often polymorphic in solution and probably for this reason have so far resisted nearly all attempts to crystallise them with metal complexes,[3,4] although nmr has been successfully used to provide elegant binding models for diruthenium complexes.[5] In that work, the binding mode of the diruthenium complex was clearly chiral, with only the Λ,Λ- enantiomer able to interact convincingly with the diagonal loop. This solution model is still the only one to define how this important class of metal complexes can interact with a unimolecular G-quadruplex, though strong 'light-switch' effects have been seen with related complex and known quadruplex-forming sequences.[6,7]

The binding mode of Λ-[Ru(TAP)$_2$(11-CN-dppz)]$^{2+}$ to duplex DNA was recently described by us[8] and showed that the inclusion of the 11-CN substituent in the dppz ligand resulted in the closing of the TC/GA terminal step, in contrast to a wealth of previous observations showing that the TA basepair was readily flipped out when adjacent to dppz at a terminal step.[9] When racemic [Ru(TAP)$_2$(11-CN-dppz)]$^{2+}$ was crystallised with d(TAGGGTTA), a G-quadruplex assembly was formed[10] in which two Λ-enantiomers were bound at each end of the G-quadruplex stack (Figure 1a). In that work, two Δ-enantiomers (not the stoichiometric equivalent, which would be four) were sandwiched between adjacent quadruplex assemblies and made little interaction with the DNA component, and two of the four 3' terminal adenine bases were not visible at all due to disorder, leading us to believe that this base was unimportant. The enantiomeric difference shown by this study reinforces the Λ preference previously reported by Thomas et al. [5] The structure also showed the stabilisation of the 5'- *syn*-guanine residues in the quadruplex assembly, leading to an overall antiparallel conformation. The disorder of the terminal adenine suggested an investigation of the truncated d(TAGGGTT) sequence might give a more reproducible crystallisation. Unexpectedly, in this work we show for the first time that the parent Λ complex (without the 11-CN dppz substituent) can stabilise a T-T mismatch pair as part of a TA/TT cavity, and also for this first time that semi-intercalation (kinking) can be seen between thymine residues, whereas up till now we have only seen such kinking induced between two guanine residues, at a GG/CC step.[11] These are structural features which are most readily observed by X-ray crystallography, although very probably detectable in solution experiments [12] and by single molecule approaches. [13] The lack of interaction with the parent dppz chromophore strongly enhances our previous observation of the surprisingly powerful effect of 11-CN substitution in these Λ enantiomers on DNA binding.

[a] *Chemistry Department, University of Reading, Whiteknights, Reading, RG6 6AD, UK*
[b] *Department of Pharmacy, University of Reading, Whiteknights, Reading, RG6 6AD, UK*
[c] *Diamond Light Source, Harwell Science and Innovation Campus, Didcot, Oxfordshire, OX11 0DE, UK.*
† Footnotes relating to the title and/or authors should appear here.
Electronic Supplementary Information (ESI) available: [details of any supplementary information available should be included here]. See DOI: 10.1039/x0xx00000x

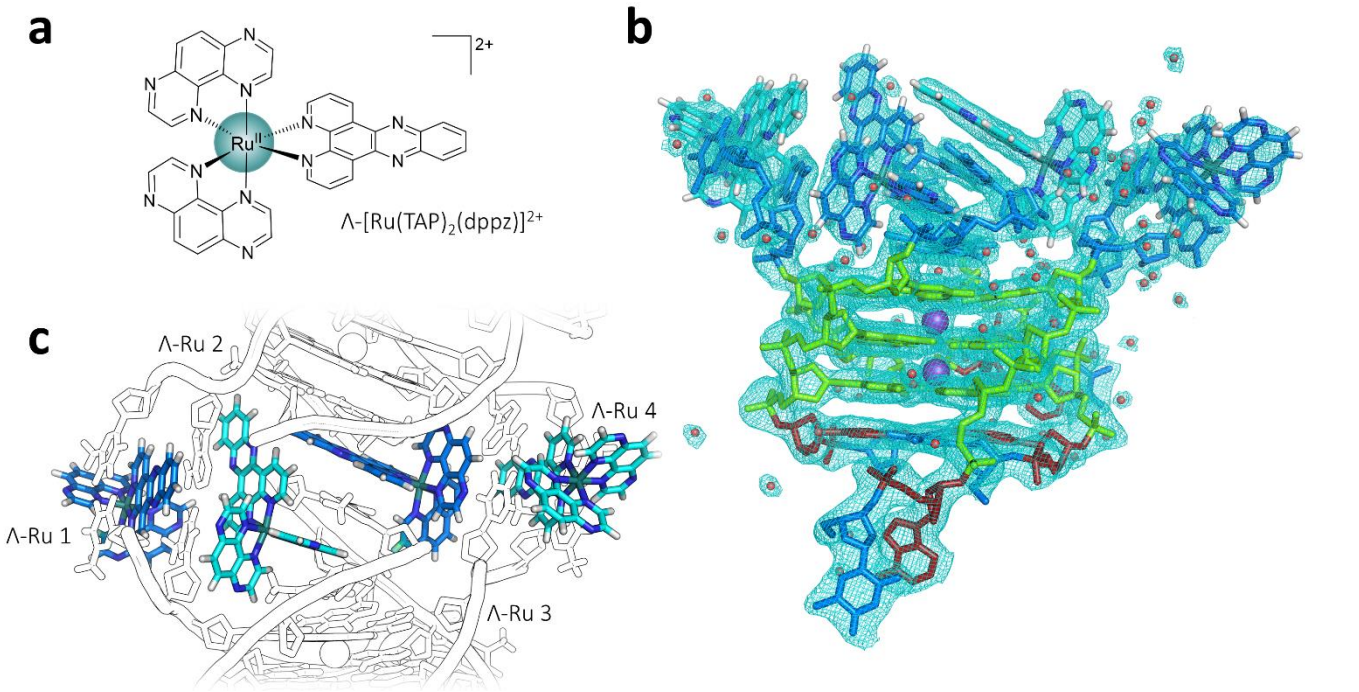

Figure 1. a) The Λ-$[Ru(TAP)_2(dppz)]^{2+}$ complex used in this study; b) Overall view of the parallel stranded asymmetric unit of the structure reported here (PDB code 6RNL). Four strand of the sequence d(TAGGGTT) assembled with two K^+ ions and four crystallographically independent Λ-$[Ru(TAP)_2(dppz)]^{2+}$ cations. Colour code for residues throughout – guanine -green; adenine- red; thymine – blue.. Alternative view are shown as Figures S1 and S2. The map is countoured at 0.29 e $Å^{-3}$ c) Generation of the four ruthenium complex environments at the interface between two nucleic acid assemblies. The numbering of the four ruthenium complexes corresponds to that usd in the text. The kink in the DNA stack is generated by one of the TAP ligands of complex Ru2, between a T-T mispair and a water-bridged T-T mispair.

The complex *rac*-$[Ru(TAP)_2(dppz)]^{2+}$ crystallised with the d(TAGGGTT) sequence and K^+ ions to give crystals containing only the lambda enantiomer (Figure 1a). The structure was phased using SAD data measured at the Ru absorption edge at 22.4 KeV. Data collection and refinement parameters are shown in Table S1. The stoichiometric ratio in the resulting crystal is 1:1, giving four complexes per tetrameric assembly. This is the same ratio as in the previous study [10] but giving an entirely different outcome. In our study of $[Ru(TAP)_2(11\text{-}CN\text{-}dppz)]^{2+}$ crystallised with d(TAGGGTTA), each of the four crystallographically independent lambda complexes had an almost identical nucleic acid environment. In this crystal structure, each complex has a distinct environment within the crystal, and none makes contact with the central G-quadruplex unit (Figure 1, b and c, and Figures S1 and S2 for alternative views). Here, we observe a parallel-stranded assembly, shown schematically in Figure 2, held together by two K^+ ions. A Na^+ ion can also be identified. (Figure 3a and b). What was unexpected is the overall bend (Figure 1c) introduced into an otherwise parallel stack by a semi-intercalative kinking motif similar to that we have we have previously observed in duplex structures. [9,11,14] The ~50° kink seen previously was always at GG steps of the sequence. Here, the kink is formed by a T-T mismatch pair and a second pair of thymine bases linked by water bridges (Figure 3c). The motif generates an overall kink angle of about 28°, as can be seen by looking at the angle generated between the G-quadruplex parts of the assembly in Figure 1c, with a local kink of 34°, measured from the thymine base planes shown in Figure 3c. The packing diagrams of the structure

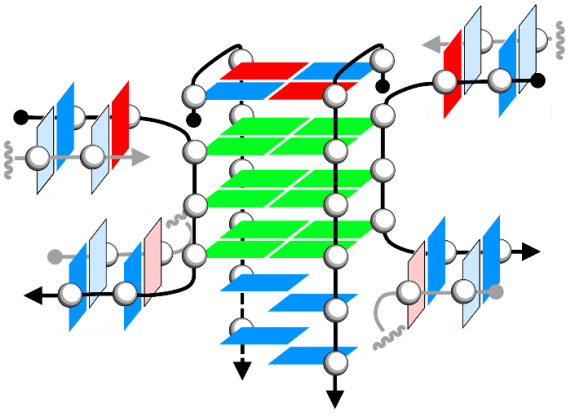

Figure 2. Structural schematic. The four strands of the sequence d(TAGGGTT) are shown with arrows in the chain direction 5'-3'. The TA and TT basepairs formed with bases from symmetry related strands have thymine as pale blue and adenine as pink.

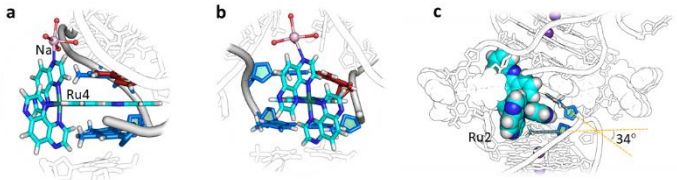

Figure 3. Structural details of TAP ligands. a) and b) coordination of a Na+ ion to a TAP ligand of Ru4 b) the local 34° kink introduced by a TAP ligand of Ru2.

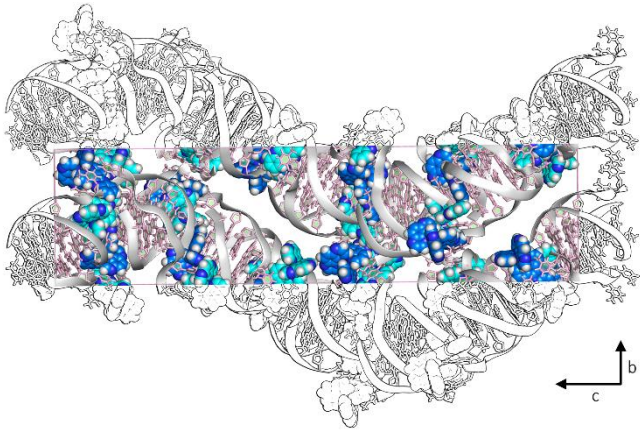

Figure 4. Packing diagram for space group $P6_5$ showing the effect of the 28° kink on the overall packing. The contents of one unit cell are shown in colour. See also Figure S3 for further packing diagrams.

viewed perpendicular to the long axis show the overall effect of this kinking on the assembly. The asymmetric units are packed together in spirals about the z direction in space group $P6_5$ (Figure 4), giving head to tail stacking and generating the four ruthenium environments observed at the interface between the units. All four crystallographically independent complexes are bound in thymine-rich environments and hence suggest comparisons with the binding of metal complexes to loop regions in single stranded DNA, as thymine-thymine mismatched base pairs are situated adjacent to, and possibly stabilised by, all of the complexes, and stacking with both the TAP and the dppz ligands. For clarity, each will be described separately, and also to this end, Figure S4 shows the asymmetric unit with two of the complexes moved to a different symmetry related position.

Two of the four complexes (Ru1 and Ru4) have almost the same environments, at the ends of the overall assembly. T1 and A2 of one strand pair with T6 and T7 of another strand, as shown in the schematic of Figure 2, to generate an intercalation cavity created by a standard AT basepair and a TT mismatch pair (Figure 5a). These binding sites also provide a model for what would be major groove binding in duplex DNA. The sites are distinguished by coordination of a Na^+ ion to one TAP ligand of Ru4 only. The ion is directly coordinated to one of the TAP ligands, and through a water bridge to a TAP ligand of Ru3. The TAP ligands in these structures have previously been observed to be hydrated,[9] and this provides a convenient rationale for the sometimes relative ease of crystallisation when compared to the more hydrophobic but isosteric and isoelectronic phen analogue, the well-known 'light-switch' complex $[Ru(phen)_2dppz]^{2+}$.[15,16] In the overall assembly the Ru1 and Ru4 cavities are end-stacked on each other, generating a quasi-continuous stack running orthogonal to the main helix axis direction, which corresponds to the b axial direction in figure 3. The additional charge neutralisation by Na^+ is possibly an additional stabilising factor for this assembly. This monovalent ion coordination may also account for the asymmetry introduced by the differing environments of Ru2 and Ru3, since there is no corresponding ion linking Ru1 and Ru2.

The environments of the two central ruthenium complexes are distinctly different, thus generating the overall lack of quasi-twofold symmetry in this structure. Ru3 appears almost completely surrounded by TA and TT basepairs, and the two faces of the complex are shown in Figures 5b and 5c. One dppz face contacts a TA/TA quartet surface formed by two T1/A2 ends, shown in Figure 4b. The other dppz surface contacts a TT mispair formed from two T7 residues, shown in Figure 4c. A further A2-T6 basepair contacts the TAP ligand shown in Figure 4b .

The environment of Ru2 is perhaps the most unexpected and as already stated above generates the kink in the overall $P6_5$ packing shown in Figures 2 and 3b. The kink is generated at one of the TAP ligands, with a T7-T7 mismatch on one side of the TAP and two thymine residues, T6 and T6, with two water bridges on the other (Figure 5d). Unexpectedly, the dppz is free, so that this complex is only held in place by this kinking interaction. This kinking site shows a remarkable overall resemblance to that seen in the original Λ-$[Ru(TAP)_2(dppz)]^{2+}$ structure, with the DNA duplex sequence $d(TCGGCGCCGA)_2$,[11] and in many structurally isomorphous examples since then.[9] In dilute solutions of B-DNA the thermodynamic binding constants

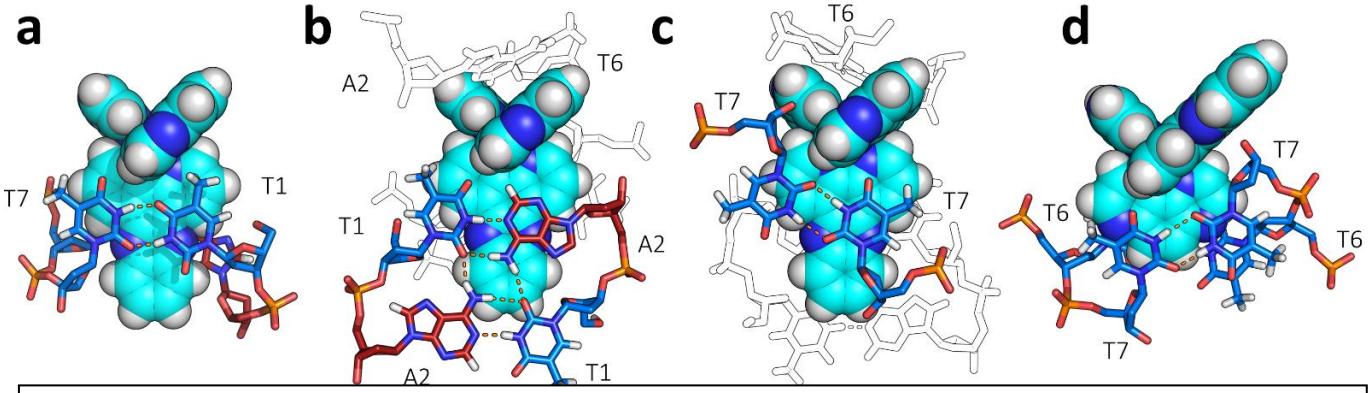

Figure 5 The ruthenium complex environments a) TT mismatch and AT match form the cavity for Ru1 and Ru4 similarly b) and c) TT mismatch cavity and additional T stacking and hydrogen bonding around Ru3 d) Kinking (semi-intercalation) at Ru2, also generated by TT mismatching. This complex is not bound by intercalation of the dppz chromophore, but just by the interaction of one of the TAP ligands as shown here. Note that all three ruthenium complex environments feature TT mismatched basepairs.

show a relatively weak interaction compared with dppz intercalation.[9] In crystals and in other tightly packed environments such as the living cell, a combination of weak interactions can lead to environments which could not be predicted from any solution study, and what we are seeing here is perhaps a model for such cases.

Both TT mismatched basepairs and kinking by phen and TAP ligands may be important components of the binding of ruthenium polypyridyl complexes to higher-order DNA structures containing loop regions. Octahedral complexes have an inherently greater potential for specific interactions than square planar ones but typically not much is known about their binding modes.[17] So far the only structural evidence is provided by the work of the Thomas group[5] as already stated. In that work (in which the ancillary ligands were bpy) the diruthenium cation threaded through a diagonal loop, with the principal interactions being with the central thymine residue of the loop. We have previously shown that, of the well known ancillary ligands in these systems, bpy is less likely to cause kinking and stacking than either phen or TAP.[18] More recently the TAP analogue of this diruthenium compound has been shown to have a range of useful properties in cell systems.[19] It was studied as an enantiomeric mixture and gave spectroscopic results clearly indicative of several binding modes. The specificity of these complexes does not just arise from end-stacking to the G-quadruplex chromophore but plausibly also includes the sort of thymine interactions revealed by the present work. There are several examples of ruthenium polypyridyl complexes which are luminescent when bound to what may well be thymine-adenine loop regions of G-quadruplexes, but there is no structural data for any of these. The binding modes seen in this work, which have no counterpart in duplex DNA, and would not be predictable from any modelling calculation, provide a useful springboard for understanding luminescence and other spectroscopic behaviour. Each of the binding modes shown in Figure 3 would have different luminescence behaviour if it were the phen analogue, based on our previous work. Ru3, being almost enclosed, would be most luminescent, with Ru1 and Ru4 expected to be similar, and Ru2 the most exposed and hence the least luminescent. A previous paper from our laboratory has considered the delta enantiomer/duplex DNA case in detail.[14]

In future work we aim to provide a comparable interpretation of the binding of lambda complexes to G-quadruplex loop regions. We would also like to understand the crucial factor which determines whether the G-quadruplex is parallel, or antiparallel as in ref 10. It is not clear how much of the switch can be ascribed to the modification of the dppz ligand and how much the crystallisation is sequence dependent.

Acknowledgements

We thank Diamond Light Source and EPSRC for a studentship (to K. McQ.) and the BBSRC for support from grant nos. BB/019250/1 and BB/M004635/1 (To CJC, JAB, JPH and DJC). We very much appreciated the provision of beamtime by Diamond Light Source on beamline I03.

References

1 G. Biffi, D. Tannahill, J. McCafferty and S. Balasubramanian, *Nat. Chem.*, 2013, **5**, 182–186.

2 S. Asamitsu, S. Obata, Z. Yu, T. Bando and H. Sugiyama, *Molecules*, 2019, **24**, 429.

3 N. H. Campbell, N. H. A. Karim, G. N. Parkinson, M. Gunaratnam, V. Petrucci, A. K. Todd, R. Vilar and S. Neidle, *J. Med. Chem.*, 2012, **55**, 209–222.

4 C. Bazzicalupi, M. Ferraroni, F. Papi, L. Massai, B. Bertrand, L. Messori, P. Gratteri and A. Casini, *Angew. Chemie - Int. Ed.*, 2016, **55**, 4256–4259.

5 T. Wilson, P. J. Costa, V. Félix, M. P. Williamson and J. A. Thomas, *J. Med. Chem.*, 2013, **56**, 8674–8683.

6 L. Xu, X. Chen, J. Wu, J. Wang, L. Ji and H. Chao, *Chem. - A Eur. J.*, 2014, **21**, 4008–4020.

7 Q. Yu, Y. Liu, C. Wang, D. Sun, X. Yang, Y. Liu and J. Liu, *PLoS One*, , DOI:10.1371/journal.pone.0050902.

8 K. McQuaid, J. P. Hall, J. A. Brazier, D. J. Cardin and C. J. Cardin, *Chem. - A Eur. J.*, 2018, **24**, 15859–15867.

9 C. J. Cardin, J. M. Kelly and S. J. Quinn, *Chem. Sci.*, 2017, **8**, 4705–4723.

10 K. McQuaid, H. Abell, S. P. Gurung, D. Allan, G. Winter, T. Sorensen, D. J. Cardin, J. A. Brazier, C. J. Cardin , J. P. Hall, *Angew. Chemie Int. Ed.*, DOI:10.1002/anie.201814502.

11 J. P. Hall, K. O'Sullivan, A. Naseer, J. A. Smith, J. M. Kelly C. J. Cardin, *Proc. Natl. Acad. Sci.*, 2011, **108**, 17610–17614.

12 P. Lincoln and B. Nordén, *J. Phys. Chem. B.*, 1998, **102**, 9583–9594.

13 W. Vanderlinden, P. J. Kolbeck, W. Frederickx, S. F. Konrad, T. Nicolaus, C. Lampe, A. S. Urban, C. Moucheron and J. Lipfert, *Chem. Commun.*, , DOI:10.1039/C9CC02838B.

14 J. P. Hall, P. M. Keane, H. Beer, K. Buchner, G. Winter, T. L. Sorensen, D. J. Cardin, J. A. Brazier and C. J. Cardin, *Nucleic Acids Res.*, 2016, **44**, 9472–9482.

15 J. P. Hall, D. Cook, S. R. Morte, P. McIntyre, K. Buchner, H. Beer, D. J. Cardin, J. A. Brazier, G. Winter, J. M. Kelly and others, *J. Am. Chem. Soc.*, 2013, **135**, 12652–12659.

16 H. Niyazi, J. P. Hall, K. O'Sullivan, G. Winter, T. Sorensen, J. M. Kelly and C. J. Cardin, *Nat. Chem.*, 2012, **4**, 621–628.

17 Q. Cao, Y. Li, E. Freisinger, P. Z. Qin, R. K. O. Sigel and Z.-W. Mao, *Inorg. Chem. Front.*, 2017, **4**, 10–32.

18 J. P. Hall, S. P. Gurung, J. Henle, P. Poidl, J. Andersson, P. Lincoln, G. Winter, T. Sorensen, D. J. Cardin, J. A. Brazier and C. J. Cardin, *Chem. - A Eur. J.*, 2017, **23**, 4981–4985.

19 S. A. Archer, A. Raza, F. Dröge, C. Robertson, A. J. Auty, D. Chekulaev, J. A. Weinstein, T. Keane, A. J. H. M. Meijer, J. W. Haycock, S. MacNeil and J. A. Thomas, *Chem. Sci.*, 2019, **2**, 3502–3513.

Supplementary information for

Three thymine-adenine binding modes of the ruthenium complex Λ-$[Ru(TAP)_2dppz]^{2+}$ to the G-quadruplex $d(TAGGGTT)_4$ shown by X-ray crystallography

Kane T. McQuaid, James P. Hall, John A. Brazier, Lena Baumgartner, David J. Cardin and Christine J. Cardin

Table S1. Data collection and refinement for the crystal structure of Λ-$[Ru(TAP)_2dppz]^{2+}$ with $d(TAGGGTT)_4$

Crystallisation Parameters	
Crystal Morphology	Hexagonal Rod
Growth Temperature (K)	291
Crystal Size (μm)	20x20x300
Growth Time	3 weeks
Data Collection	
Beamline	I03
X-Ray Wavelength (Å)	0.557
Transmission (%)	40.01
Beamsize (μm)	50x20
Exposure Time (s)	0.05
Nº Images/Oscillation (º)	3600/0.10
Space Group	$P6_5$
Cell Dimensions *a*, *b*, *c* (Å)	38.53, 38.53, 128.77; 90, 90, 90
Data Processing	
Resolution (Å)	32.29 - 1.88 (1.91 - 1.88)
R_{merge}	0.120 (3.986)
R_{meas}	0.1233 (3.986)
R_{pim}	0.027 (1.003)
№ Observations	175,231 (7823)
№ Unique Observations	8849 (465)
I/σI	14.3 (0.7)
$CC_{1/2}$	0.999 (0.585)
Completeness (%)	100.00 (100.00)
Multiplicity	19.8 (16.8)
Mid-slope of anom normal probability	1.246
* Outer Shell Statistics Shown in Parentheses	
Refinement	
Phase Solution Method	SAD
Resolution	32.3 (1.88)
No. of Reflections	8708
R_{work}/R_{free}	0.1872/0.2145
No. of Atoms	
DNA	576
Metal Complex	204
Water	75

Average B Factors (Å^2)	
DNA	44.16
Metal Complex	42.62
Water	40.21
rmsd	
Bond Lengths (Å)	0.013
Bond Angles (o)	1.0
PDB ID	**6RNL**

Figure S1. Alternative view of the asymmetric unit of 6RNL, showing $2F_o$-F_c density map, contoured at 0.29 e Å^{-3}

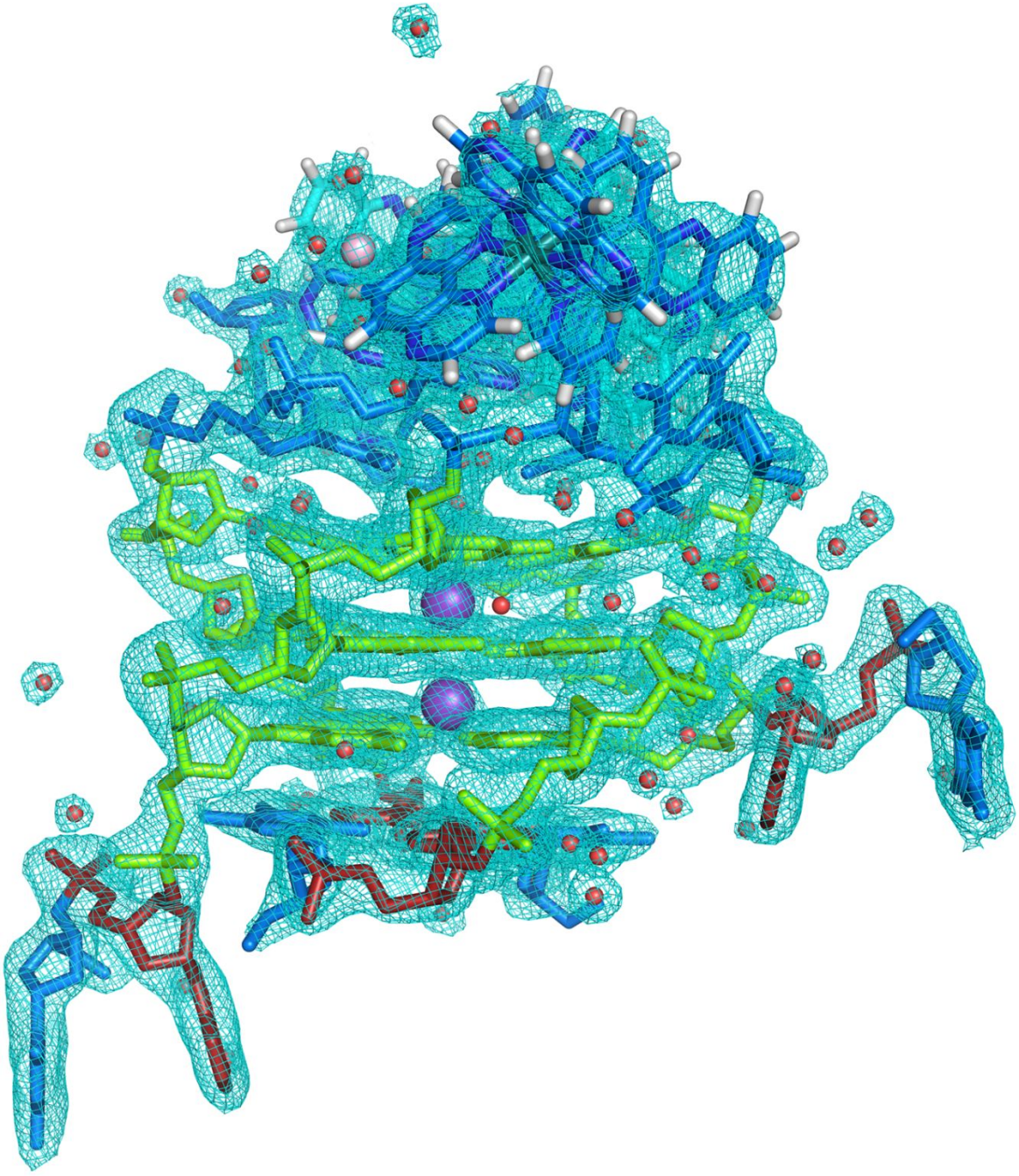

Figure S2. 6RNL showing the water molecules.

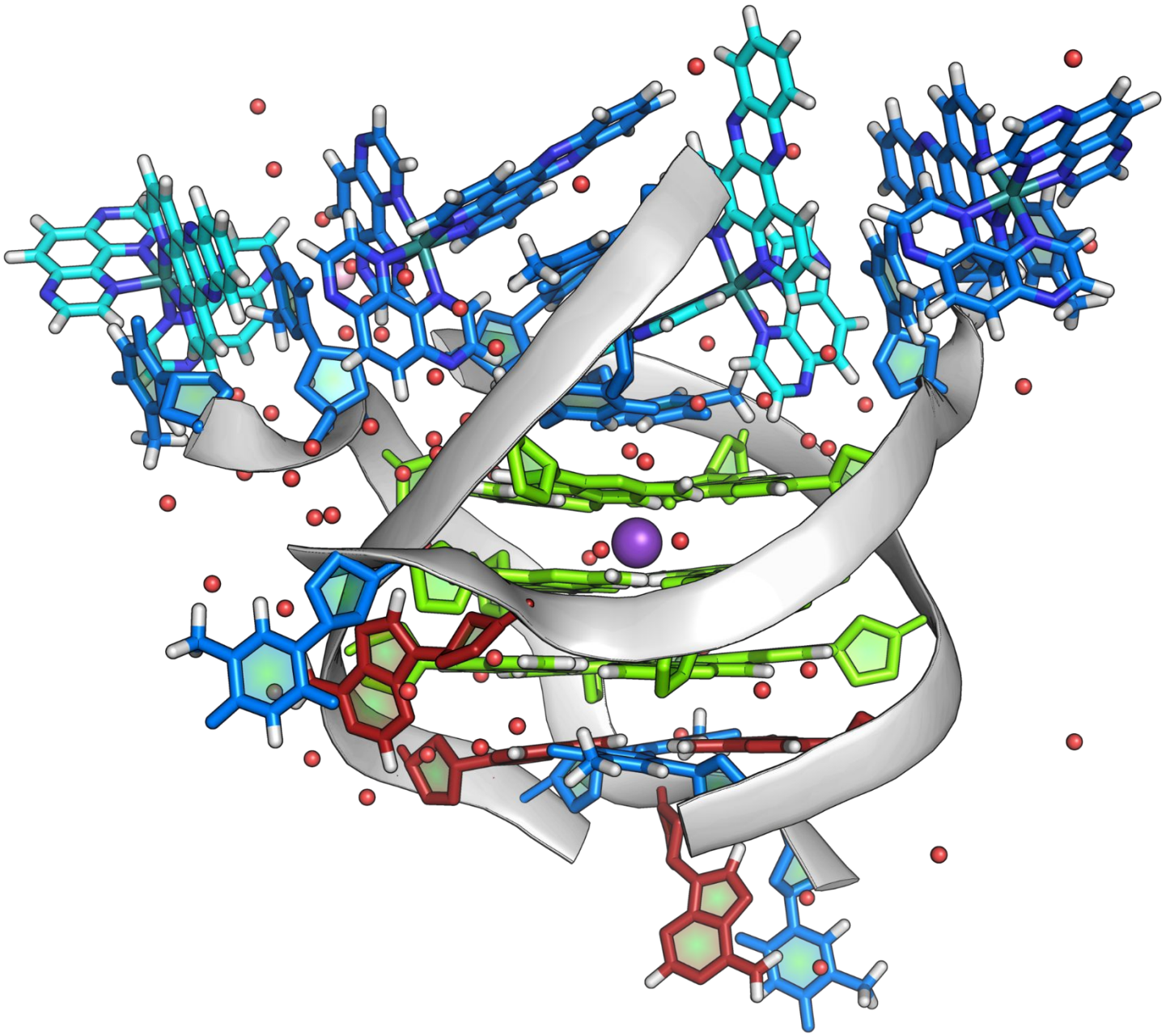

Figure S3 Two view of the crystal packing in space group $P6_5$

a) Perpendicular to the c-axis, with a axis vertical.

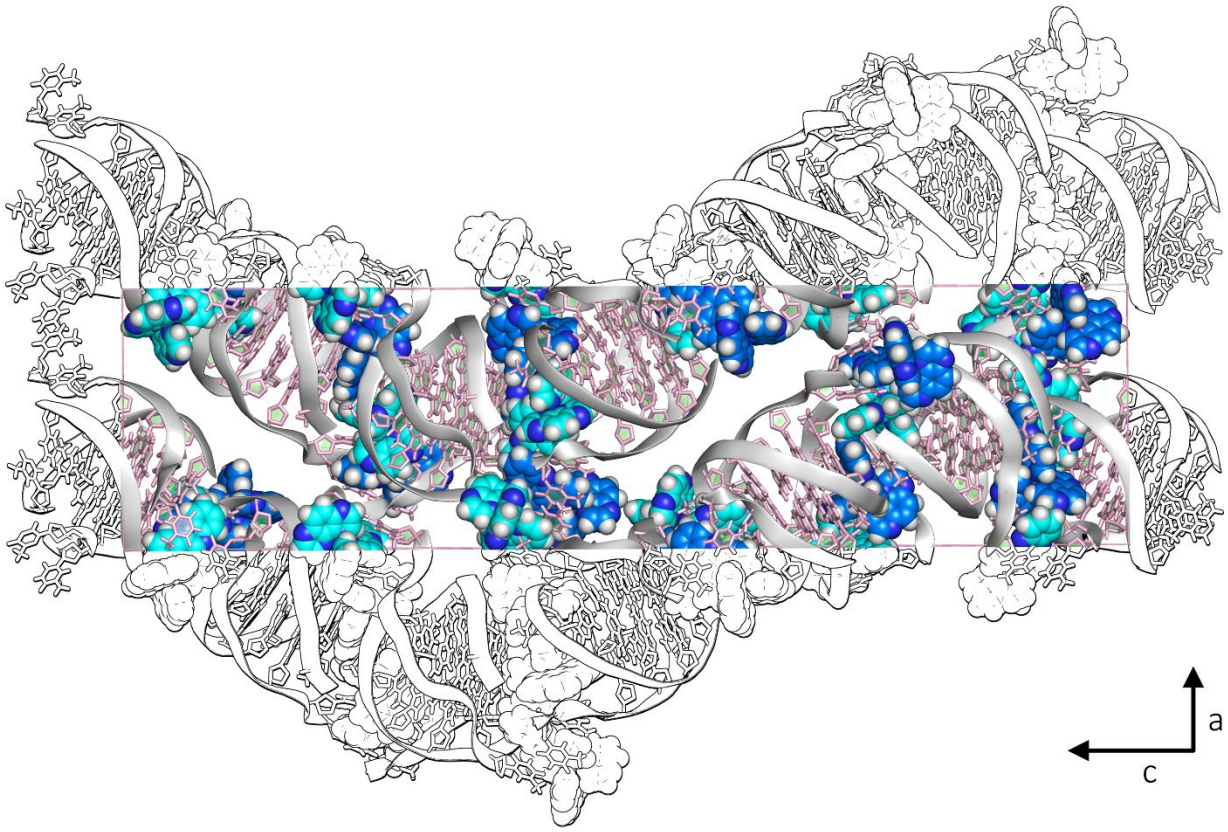

b) Projection down the c axial direction.

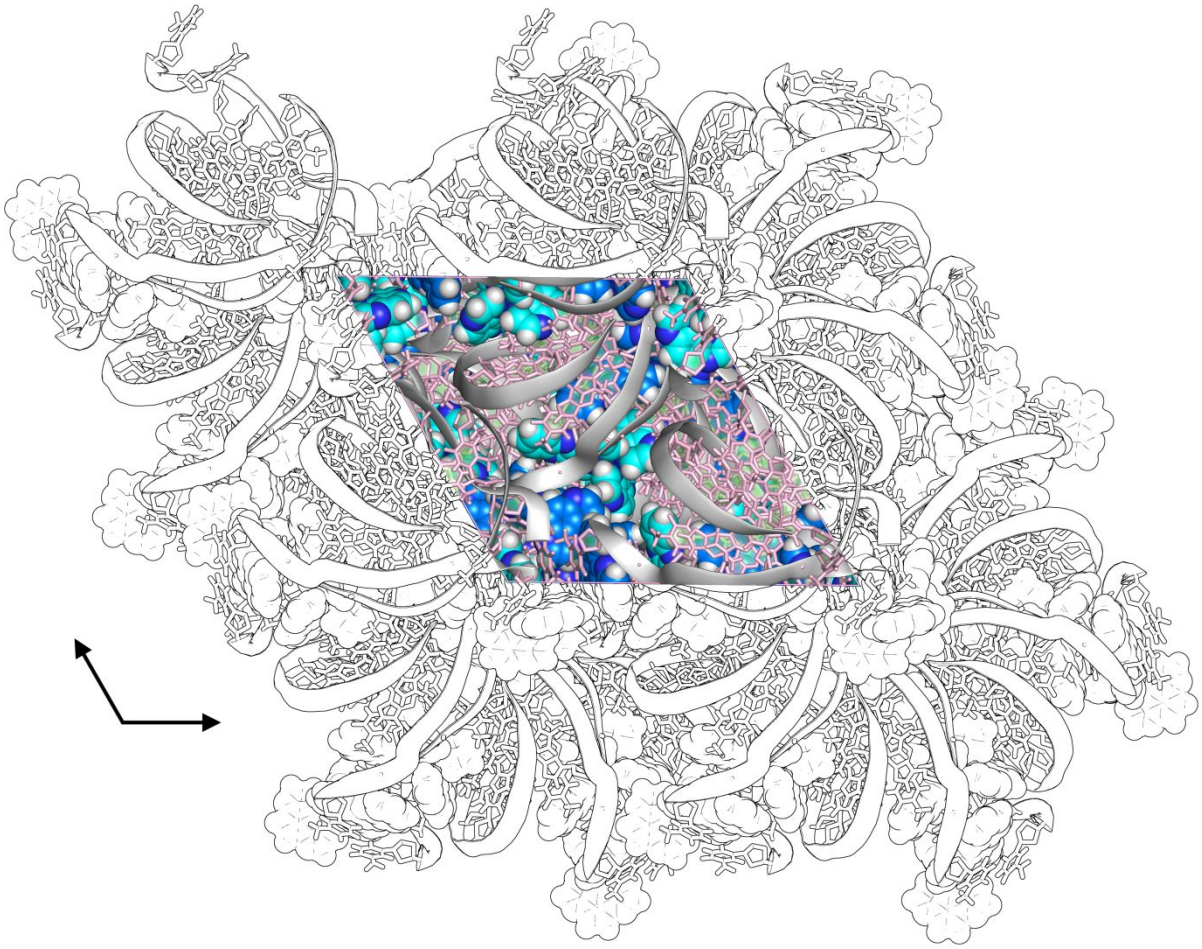

Figure S4

The complex binding modes shown in two orientations, and clarified by moving two of the complexes to a different asymmetric unit.

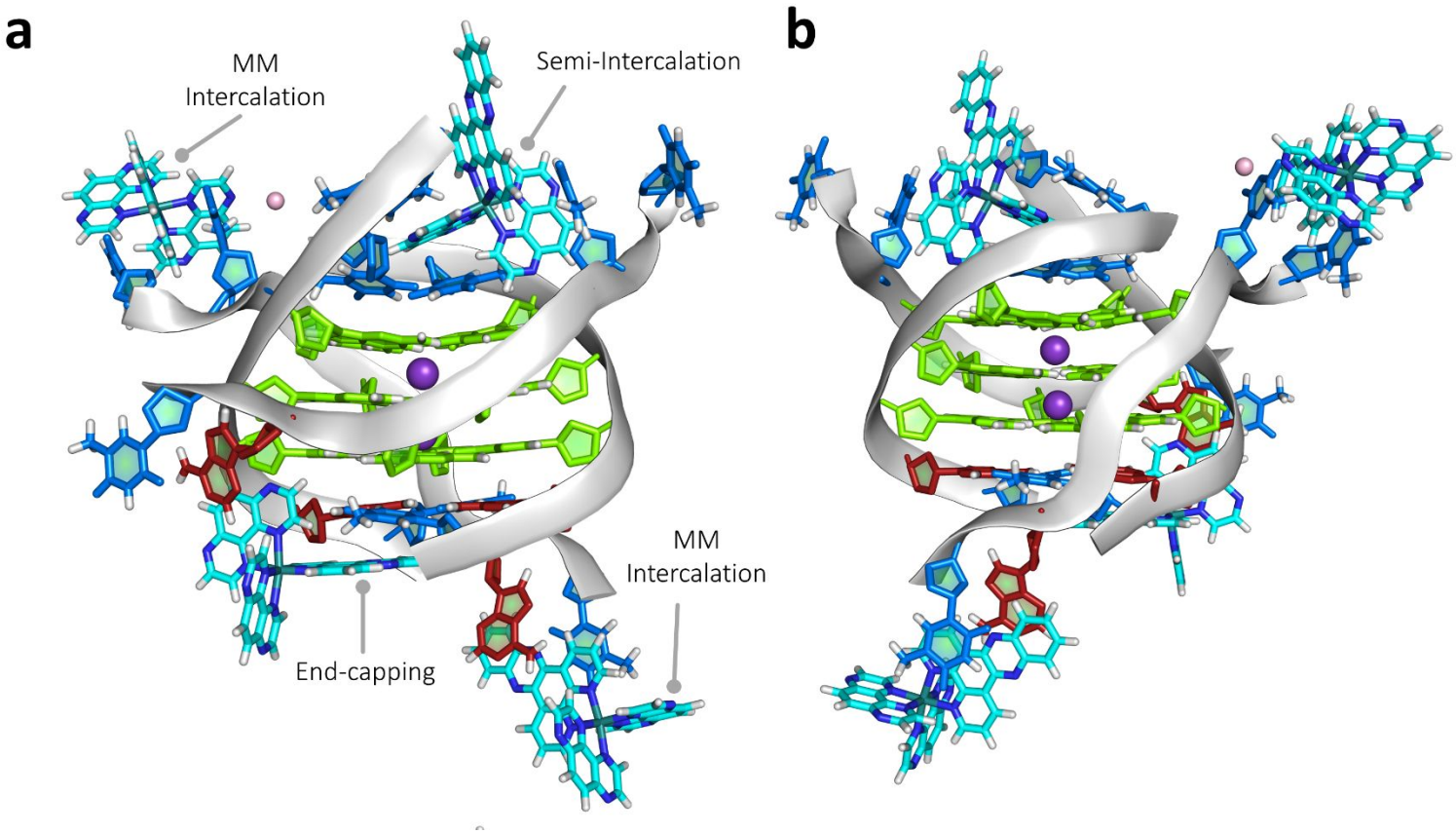

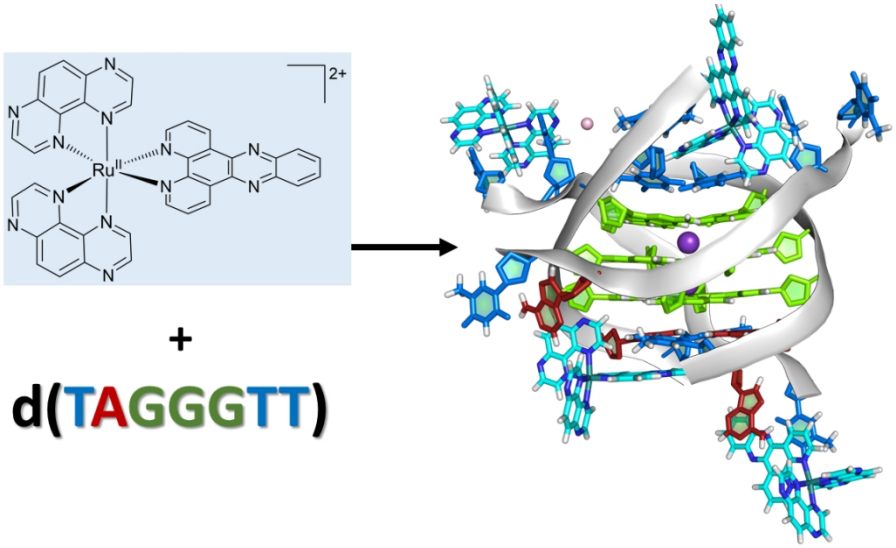
2+
Ru
+
d(TAGGGTT)